I S A V

Journal of Theoretical and Applied

Vibration and Acoustics

10th International Conference on Acoustics and Vibration
journal homepage: http://tava.isav.ir

Vibrational energy harvesting from a monostable piezomagnetoelastic structure with multi-frequency excitation

Hadi Partovi Aria [a], **Arash Bahrami** [b,*], **Ali Sadighi** [b]

[a] *M.Sc. Student, School of Mechanical Engineering, College of Engineering, University of Tehran, Tehran, Iran*

[b] *Assistant Professor, School of Mechanical Engineering, College of Engineering, University of Tehran, Tehran, Iran.*

Invited paper

ARTICLE INFO

Article history:
Received 20 March 2020

Received in revised form 12 May 2020

Accepted 10 December 2020

Available online 20 December 2020

Keywords:
Energy harvesting

Multi-frequency excitation

Nonlinear dynamics

Piezomagnetoelastic

ABSTRACT

The present article proposes the idea of multi-frequency excitation to harvest energy from low-frequency ambient vibrations. A nonlinear piezomagnetoelastic set-up, operating in the monostable mode, is considered. Due to nonlinearities being present in the system, a multi-frequency excitation gives rise to complicated phenomena such as combination and simultaneous resonances. We propose the idea of multi-frequency excitation and employing secondary resonances such as combination and simultaneous resonances occurring in nonlinear systems. Nonlinear differential equations governing the harvester dynamics are obtained based on the Hamilton extended principle and solved using the direct harmonic balance method. Numerical results are presented for an actual energy harvester subjected to a dual-frequency excitation. It is ascertained that multi-frequency excitation and exploiting combination and simultaneous resonance result in a significant enhancement in the harvester output voltage and power. It is also found that simultaneous resonance is more effective in improving the harvester performance than combination resonances.

1. Introduction

Harvesting ambient energy through different mechanisms has attracted significant attention over the past few years. Vibrational energy harvesting has been already recognized as a standard way to provide the power required for low-power devices such as mobiles and wireless electronics [1], data transmitters [2], medical implants[3-5], and many other applications. Some technical

* Corresponding author:
E-mail address: arash.bahrami@ut.ac.ir (A. Bahrami)

Selection and peer-review under responsibility of the Iranian Society of Acoustics and Vibration of the 10th International Conference on Acoustics and Vibration
http://dx.doi.org/10.22064/TAVA.2021.533544.1188

problems like wiring complexities are lessened, and also the frequent need for changing batteries is removed by using energy harvesting as a power source[6, 7].

A variety of smart materials have been utilized so far to convert vibrational energy into electricity, including piezoelectric, electromagnetic, and electrostatic[8]. Due to their outstanding performance and efficiency, piezoelectric materials have been extensively used to capture energy from environmental vibrations, and therefore, piezoelectric transducers have received great attention [9-11].

Initial studies on vibrational energy harvesting were focused on linear systems. The common structure for harvesters consists of a cantilever beam with piezoelectric patches attached near its clamped end and external environmental excitations applied at the beam base. When the system experiences a base excitation, the vibrational energy of the system is harvested through a voltage difference across the piezoelectric layers [12]. This mechanism can also be easily implemented in practice. The major issue with the linear mechanism is that the fundamental frequency of the harvester system should be close to the excitation frequency (i.e., frequency of ambient vibration) to generate a considerable response amplitude. Consequently, linear devices offer only a narrow frequency bandwidth for energy harvesting. Therefore, tuning a linear energy harvesting device to operate near its natural frequency can be very challenging and, in some cases, impractical, especially outside the laboratory[13]. Thus, some researchers started to implement different methods to resolve this issue. Employing nonlinear phenomena could be a way to resolve the bandwidth problem [14]. Considering nonlinearities provides us with the opportunity of gaining large amplitude responses in a wider range of frequencies. Consequently, many researchers have used nonlinearities as means to enhance the revenue of energy harvesting devices under broadband excitations [13, 15].

The structure studied in the present paper is a well-known nonlinear structure in which forces between magnets are nonlinear. This structure was first studied by Moon and Holmes in 1979 [16]. They showed that the system can have different numbers of stable points and may exhibit different dynamical responses such as chaos and limit cycle oscillations. Later on, Erturk and Inman attached piezoelectric layers near the fixed end of the beam to harvest its vibrational energy [17]. They also studied the piezomagnetoelastic energy harvester in the monostable mode and used multiple scales to determine the system's response at the primary resonance[18]. Karami and Inman[19] have used the perturbation method to investigate small-amplitude oscillations of the system near its stable equilibrium points. All these studies concentrated on only a single frequency excitation around the natural frequency of the system.

In this paper, we develop a theoretical framework for a piezomagnetoelastic energy harvester operating based on multi-frequency excitation. To this end, we assume that the environmental vibrations involve two frequencies. In nonlinear systems subjected to multi-frequency excitations, new types of resonances referred to as secondary resonances may take place for certain values of excitation frequencies. Using secondary resonances, including combination and simultaneous resonances, we propose a novel nonlinear harvesting technique to enhance harvester performance. The proposed scheme is implemented in the monostable mode. In the following, we present the main formulation, and then we use the direct harmonic balance method [20] to solve the energy harvesting problem. In addition, different cases of combination resonance are compared numerically. Simultaneous resonances are also considered, and output voltage and power are determined through several numerical examples.

2. Nonlinear modeling and governing equations

2.1.Mathematical model

In this section, we employ the Hamilton extended principle to determine nonlinear initial-boundary value problem governing the harvester dynamics. Equations are obtained based on Euler-Bernoulli beam assumptions and infinitesimal strain theory. The schematic of the piezoelectric energy harvester device is illustrated in Fig. 1. The cantilever consists of an electrically neutral substrate material with symmetric electroelastic laminates uniformly coated on either side such that the neutral axis of the deflection passes through the center of the substrate. This configuration is commonly referred to as a bimorph. A tip mass is typically secured at the beam-free end to tune the mechanical resonance. Tip mass *A*, which has magnetic properties, is located opposed to two fixed magnets *B* and *C* facing each other in such a way that identical poles are opposite to each other. The cantilever beam is subjected to a harmonic base displacement [16]. The nonlinear magnetic force arising between the magnets leads to complex nonlinear behavior.

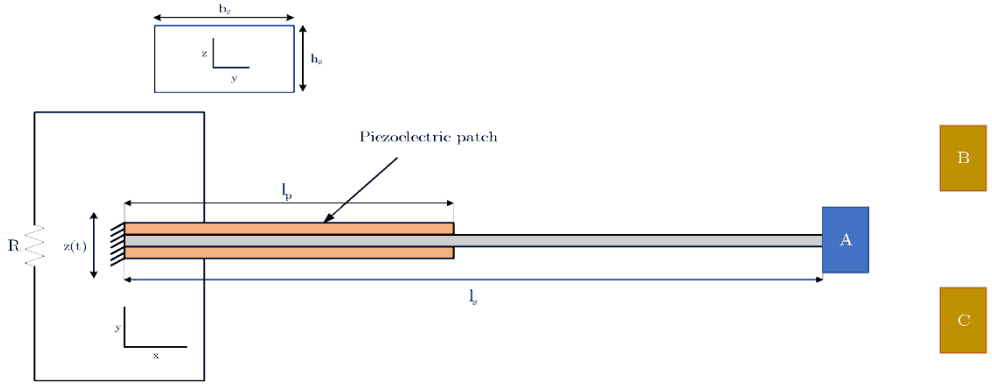

Fig 1. The schematic of the device

The kinetic energy of the beam without considering piezoelectric layers may be written as:

$$T_s = \frac{1}{2}\rho_s A_s \int_0^{l_s} [\dot{w}(x,t) + \dot{z}(t)]^2 dx \tag{1}$$

and for the piezoelectric layers

$$T_p = \frac{1}{2}\rho_p A_p \int_0^{l_p} [\dot{w}(x,t) + \dot{z}(t)]^2 dx \tag{2}$$

where $z(t)$ denotes the base displacement and $w(x,t)$ represents the beam deflection. Furthermore, ρ_s, A_s, and l_s indicate the substrate density, cross-sectional area, and cantilever length, respectively. Similarly, ρ_p, A_p, and l_p denote the corresponding values for the piezoelectric layer. With the point-mass approximation, kinetic energy for the tip mass is obtained as:

$$T_m = \frac{1}{2} M_t [\dot{w}(x,t) + \dot{z}(t)]^2 \tag{3}$$

where M_t indicates the tip mass. The potential energy of the cantilever is given by[21].

$$U_s = \frac{1}{2} E_s I_s \int_0^{l_s} [w''(x,t)]^2 dx \tag{4}$$

where E_s is the substrate Young's modulus and $I_s = bh_s^3/12$ is the cross-section second moment of area (b_s is width and h_s is the thickness of the cantilever). Also, potential energy for the piezoelectric patch is given by[22]:

$$U_p = E_p I_p \int_0^{l_p} [w''(x,t)]^2 dx - \frac{1}{2} e_{yx} b_p (h_p + h_s) \dot{\lambda}(t) w'(l,t) - \frac{1}{4} C_p [\dot{\lambda}(t)]^2 \tag{5}$$

where e_{yx} is piezoelectric constant and E_p is Young's module of the piezoelectric patch. In addition, Cp is the capacitance through one layer, defined as $C_p = b_p \varepsilon_{yy}^s l_p / h_p$. Parameters λ, bp, hp, and ε_{yy}^s indicate electrical flux, the width of the piezoelectric patch, piezoelectric thickness, and dielectric constant, respectively. The piezoelectric second moment of area is given by:

$$I_p = \frac{b_p h_p (4h_p^2 + 6h_p h_s + 3h_s^2)}{12} \tag{6}$$

The magnetic potential function may also be approximated by the following fourth-order polynomial [23]:

$$U_M = \frac{1}{2} \alpha [w(l_s,t)]^2 + \frac{1}{4} \beta [w(l_s,t)]^4 \tag{7}$$

with α and β being constant coefficients. Then equations (1)-(7) are substituted in the Hamilton extended principle to determine the following differential equations governing the cantilever vibrations:

$$\begin{cases} (\rho_s A_s + 2\rho_p A_p)\ddot{w}_1 + c\dot{w}_1 + (E_s I_s + 2E_p I_p) w_1^{iv} = -(\rho_s A_s + 2\rho_p A_p)\ddot{z} \\ \frac{1}{2} C_p \dot{v} + \frac{1}{R} v + \theta \dot{w}_1(l_p,t) = 0 \\ \rho_s A_s \ddot{w}_2 + c\dot{w}_2 + E_s I_s w_2^{iv} = -\rho_s A_s \ddot{z} \end{cases} \tag{8}$$

Here, w_1 is the deflection of the beam where the piezoelectric layers are attached, and w_2 is the deflection of the rest of the beam. Also, θ is defined as $\theta = \frac{1}{2} e_{yx} b_p (h_p + h_s)$. We also note that $\dot{\lambda}$ is equal to v. In addition, c is the damping coefficient per length. Boundary conditions are also obtained as:

$$\begin{cases} w_1(0,t) = 0 \\ \dfrac{\partial w_1(0,t)}{\partial x} = 0 \\ w_1(l_p,t) = w_2(l_p,t) \\ \dfrac{\partial w_1(l_p,t)}{\partial x} = \dfrac{\partial w_2(l_p,t)}{\partial x} \\ (E_sI_s + 2E_pI_p)\left(\dfrac{\partial^2 w_1(l_p,t)}{\partial x^2}\right) = \theta v + E_sI_s\left(\dfrac{\partial^2 w_2(l_p,t)}{\partial x^2}\right) \\ (E_sI_s + 2E_pI_p)\left(\dfrac{\partial^3 w_1(l_p,t)}{\partial x^3}\right) = E_sI_s\left(\dfrac{\partial^3 w_2(l_p,t)}{\partial x^3}\right) \\ E_sI_s\left(\dfrac{\partial^2 w_2(l_s,t)}{\partial x^2}\right) = 0 \\ E_sI_s\left(\dfrac{\partial^3 w_2(l_s,t)}{\partial x^3}\right) = M_t(\ddot{w}_2 + \ddot{z}) + \alpha w_2(l_s,t) + \beta w_2(l_s,t)^3 \end{cases} \tag{9}$$

2.2. Direct Harmonic Balance Method

Here, we employ the direct harmonic balance method [20] to solve partial differential equations and associated boundary conditions given by Eqs. (8) and (9) without discretization. Due to cubic nonlinearity showing up in the boundary conditions, combination resonances occur when $\omega_0 = |2\Omega_i \pm \Omega_j|$, where ω_0 is the fundamental frequency of the system and Ω_i (i = 1,2) are excitation frequencies [24]. Considering the base excitation includes two frequencies $z = e_1\cos(\Omega_1 t) + e_2\cos(\Omega_2 t)$, where e1 and e2 are amplitudes of excitation, the response is assumed to be in the following form

$$\begin{aligned} w_1(x,t) &= p_1(x) + q_1(x)\cos(\Omega_1 t) + h_1(x)\sin(\Omega_1 t) + m_1(x)\cos(\Omega_2 t) + n_1(x)\sin(\Omega_2 t) \\ &\quad + r_1(x)\cos(|\Omega_1 \pm 2\Omega_2|t) + t_1(x)\sin(|\Omega_1 \pm 2\Omega_2|t) \\ w_2(x,t) &= p_2(x) + q_2(x)\cos(\Omega_1 t) + h_2(x)\sin(\Omega_1 t) + m_2(x)\cos(\Omega_2 t) + n_2(x)\sin(\Omega_2 t) \\ &\quad + r_2(x)\cos(|\Omega_1 \pm 2\Omega_2|t) + t_2(x)\sin(|\Omega_1 \pm 2\Omega_2|t) \\ v(t) &= j\cos(\Omega_1 t) + k\sin(\Omega_1 t) + l\cos(\Omega_2 t) + g\sin(\Omega_2 t) + f\cos(|\Omega_1 \pm 2\Omega_2|t) + d\sin(|\Omega_1 \\ &\quad \pm 2\Omega_2|t) \end{aligned} \tag{10}$$

The response given by Eq. (10) is substituted into governing Eq. (8) and corresponding boundary conditions Eq. (9). Separating the coefficient of sin and cos terms yields a set of linear ordinary differential equations in terms of spatial variable *x* and a set of algebraic equations for boundary conditions. The response is determined by solving the linear ODE system with the boundary conditions, (for more details, see [20]).

3. Numerical Results

For numerical simulations, we use the mechanical and electrical properties of an actual harvester device, presented in Table 1 [25]. Depending on the distance between the permanent magnets and the cantilever free end, the harvester device might have different numbers of stable points and therefore exhibit different nonlinear behavior [16]. Here the distance between the magnets is

chosen so that the system has a single stable point. Such a system is called monostable. To obtain magnetic potential, we use the same method as Stanton [21]. However, we use two magnets; hence, the effect of magnet C on A is also considered. The total potential energy of the system is shown in Fig 2. for d = 20 mm and the horizontal distance s = 75 mm. the mechanical and electrical properties of the system used in the present investigation [25].

Table1. Properties of the harvester device

Parameter	Value	Unit
E_s	200	GPa
E_p	67	GPa
l_s	127	mm
l_p	38.1	mm
b_s	25.4	mm
b_p	20.574	mm
h_s	0.254	mm
h_p	0.254	mm
ρ_s	7850	Kg/m^3
ρ_p	7800	Kg/m^3
c	1.5	Ns/m
M_t	0.048	Kg
R	200	KΩ
B_r	1.4	T
V_A	1.01×10^{-5}	m^3
V_C & V_B	2.04×10^{-6}	m^3
e_{yx}	-10.4	C/m^2
ε_{yy}^{s}	$1600\varepsilon_0$	F/m
ε_0	8.854×10^{-12}	F/m

The magnetic potential function, depicted in Fig. 2, can be approximated with the following polynomial function

$$U_m = 1494[w(l_s,t)]^4 - 7.7760[w(l_s,t)]^2 + 0.01102 \quad (11)$$

where $w(l_s,t)$ signifies the free end deflection of the beam. By differentiating the magnetic potential, the applied magnetic force is obtained, and the corresponding coefficients used in the last boundary condition (i.e., the nonlinear boundary condition) are also determined.

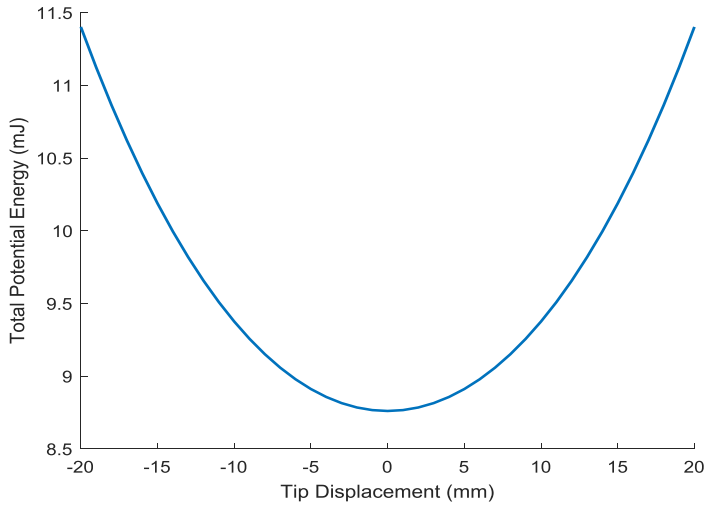

Fig 2. Total potential energy for the monostable harvester

Utilizing the numerical values tabulated in Table 1, the first natural frequency of the harvester is obtained, which is equal to 2.1 Hz. In the present investigation, we consider four different excitation schemes for which the combination resonance occurs. As mentioned earlier, the combination resonance takes place when the fundamental frequency of the system satisfies $\omega_0 = |2\Omega_i \pm \Omega_j|$. Deflection of the free end, the output voltage, and the harvested power are displayed in Fig. 3(a) through 3(c), respectively, for different combination resonance cases. Moreover, RMS voltage values are presented in Table 2 for these cases.

As both Fig. 3 and Table 2 imply, distinct excitation schemes lead to significantly different harvested power. It is observed that for excitations satisfying $2\Omega_1 - \Omega_2 = \omega_0$ and $\Omega_1 - 2\Omega_2 = \omega_0$, the amount of harvested energy is much higher than other two cases (i.e., $\Omega_1 + 2\Omega_2 = \omega_0$ and $2\Omega_1 + \Omega_2 = \omega_0$). It transpires that the highest RMS of the output voltage is obtained when the difference of the first excitation frequency and twice the second excitation frequency is equal to the fundamental frequency of the system. On the other hand, the lowest RMS voltage occurs when the sum of the first excitation frequency and twice the second excitation frequency becomes equal to the fundamental frequency.

Table 2. RMS voltages for different cases of combination resonances

Excitation scheme	RMS voltage (v)
$\Omega_1 - 2\Omega_2 = \omega_0$	2.0810
$\Omega_1 + 2\Omega_2 = \omega_0$	0.0176
$2\Omega_1 - \Omega_2 = \omega_0$	1.9645
$2\Omega_1 + \Omega_2 = \omega_0$	0.0466

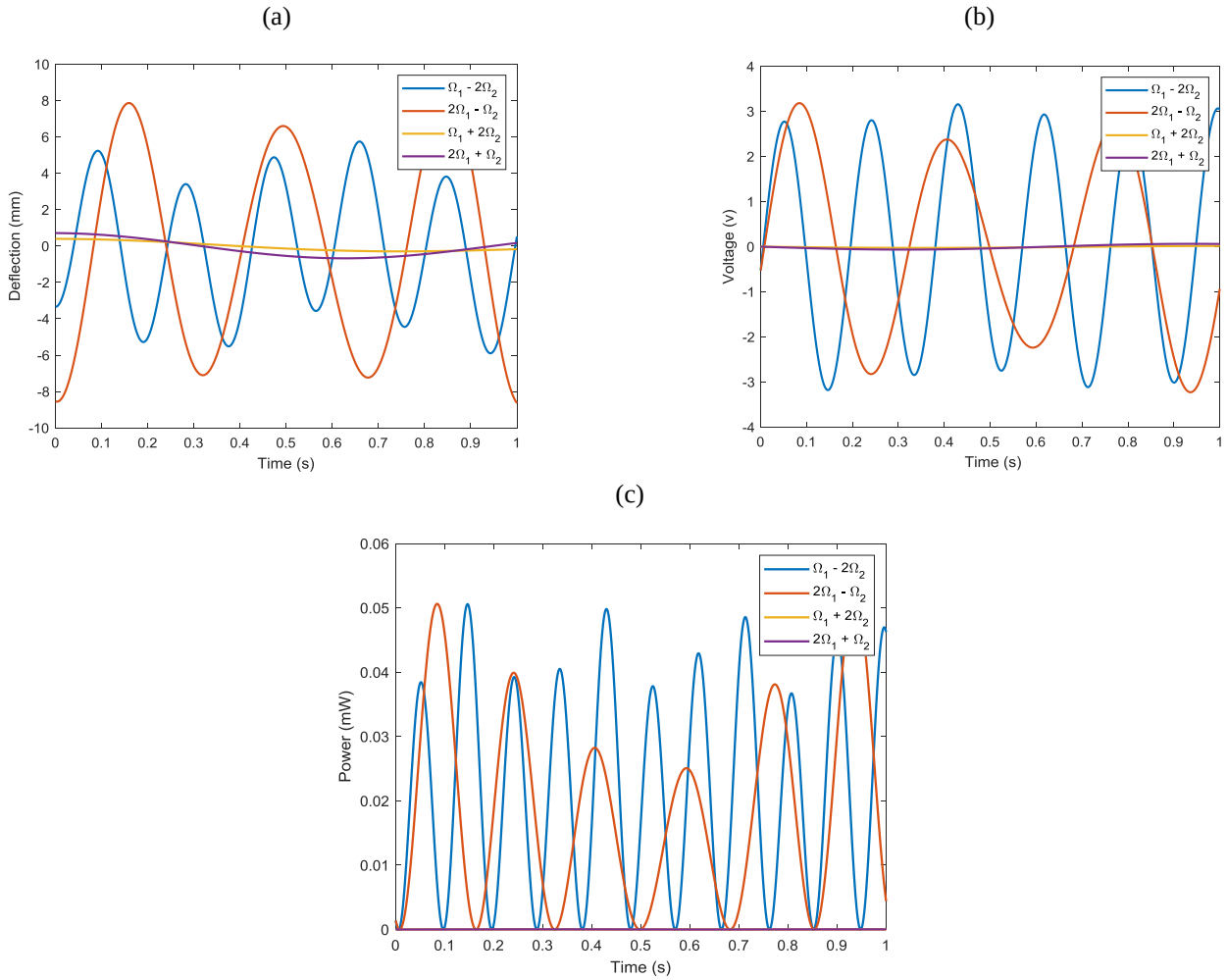

Fig 3. A comparison between different cases of combination resonances for excitation amplitudes e_1 = 0.4 cm and e_2 = 0.1 cm. (a) free end deflection (b) voltage and (c) power

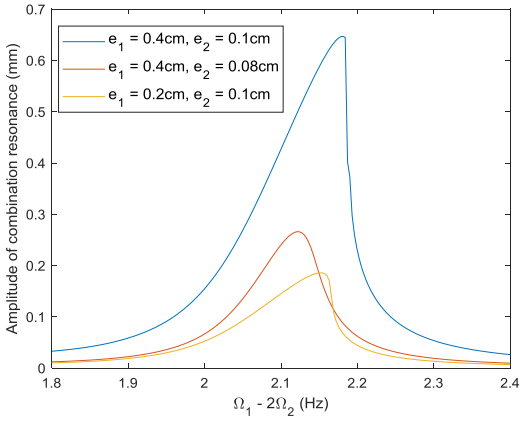

Fig 4. The frequency response curve for $\Omega_1 - 2\Omega_2 = \omega_0$ for different excitation amplitudes

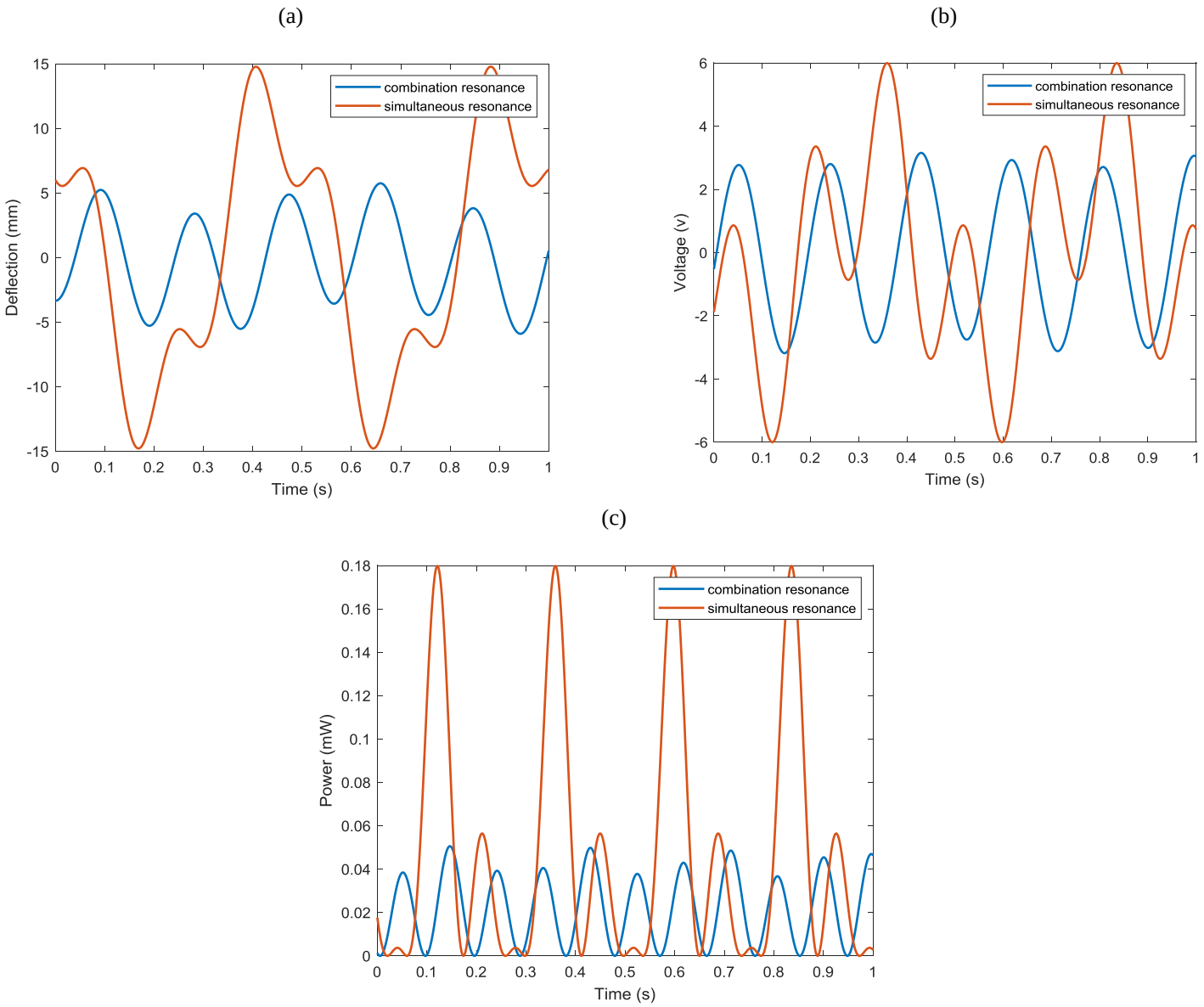

Fig 5. A comparison between combination and simultaneous resonances for excitation amplitudes e1 = 0.4 cm and e2 = 0.1 cm. (a) free end deflection (b) voltage, and (c) power

For a closer examination, we focus on the excitation scheme leading to the highest RMS output voltage (i.e., $\Omega_1 - 2\Omega_2 = \omega_0$) and plot the frequency-response curve for this case in Fig 4. As seen in this figure, the response amplitude increases with excitation amplitudes. In addition, the hardening behavior owing to cubic nonlinearity is clearly observed in the figure.

Next, we consider the excitation scheme with the largest RMS output voltage again, and this time we study another type of secondary resonances referred to as the simultaneous resonance. The simultaneous resonance occurs when two different resonances arise simultaneously in the nonlinear system. For the system under consideration, the fundamental frequency of the system is 2.1 Hz. Therefore, if the first excitation frequency is set to be $\Omega_1 = 6.3$ Hz, and the second

excitation frequency is set to be $\Omega_2 = 2.1$ Hz, then $\Omega_1 - 2\Omega_2 = \omega_0$ and hence the combination resonance is activated as same as the primary resonance because Ω_1 equals to the system fundamental frequency. Since the primary resonance coincides with a combination resonance, the resonance is called the simultaneous resonance. Fig 5 (a)- 5(c) illustrate the response of the harvester to excitation schemes leading to combination and simultaneous resonances on the same axes. As demonstrated in the figure, in compared to the combination resonance, the simultaneous resonance exhibits higher output values of voltage, power, and deflection. Moreover, the RMS output voltage corresponding to the simultaneous resonance is determined to be 3.087 v which is 48.3% higher than that of the combination resonance.

4. Conclusion

In this research, a monostable piezomagnetoelastic structure for energy harvesting has been studied. We assumed that the system was subjected to a multi-frequency excitation. To solve the nonlinear initial-boundary value problem governing the harvester dynamics, a semi-analytical solution has been developed based on the direct harmonic balance method. The output voltage and harvested power have been determined for various combination resonances and simultaneous resonance. The effect of excitation amplitude on the frequency response curve for the combination resonance amplitude has also been investigated. In addition, output RMS voltages for these cases have been obtained. It was found out that employing nonlinear resonance, including combination and simultaneous resonances, may effectively increase the amount of harvested energy. Numerical investigations performed for the present harvester subjected to various combination resonances demonstrated that employing the convenient excitation scheme leads to a significant enhancement in the output voltage and power. In addition, for the excitation scheme leading to simultaneous resonance, when both a combination resonance and the primary resonance occur simultaneously, the performance improvement is quite remarkable.

References

[1] J.A. Paradiso, T. Starner, Energy scavenging for mobile and wireless electronics, IEEE Pervasive computing, 4 (2005) 18-27.
[2] J.-W. Kim, H. Takao, K. Sawada, M. Ishida, Integrated inductors for RF transmitters in CMOS/MEMS smart microsensor systems, Sensors, 7 (2007) 1387-1398.
[3] E. Romero, Energy Harvesting for Powering Biomedical Devices, in: International Conference on Nanochannels, Microchannels, and Minichannels, American Society of Mechanical Engineers, 2012, pp. 23-27.
[4] M.H. Ansari, M.A. Karami, A sub-cc nonlinear piezoelectric energy harvester for powering leadless pacemakers, Journal of intelligent material systems and structures, 29 (2018) 438-445.
[5] A. Zurbuchen, A. Haeberlin, L. Bereuter, A. Pfenniger, S. Bosshard, M. Kernen, P.P. Heinisch, J. Fuhrer, R. Vogel, Endocardial energy harvesting by electromagnetic induction, IEEE transactions on biomedical engineering, 65 (2017) 424-430.
[6] W.W. Clark, C. Mo, Piezoelectric energy harvesting for bio mems applications, in: Energy Harvesting Technologies, Springer, 2009, pp. 405-430.

[7] A.C. Galbier, M.A. Karami, A bistable piezoelectric energy harvester with an elastic magnifier for applications in medical pacemakers, in: Smart Materials, Adaptive Structures and Intelligent Systems, American Society of Mechanical Engineers, 2016, pp. V002T007A008.
[8] S. Priya, D.J. Inman, Energy harvesting technologies, Springer, 2009.
[9] S.R. Anton, H.A. Sodano, A review of power harvesting using piezoelectric materials (2003–2006), Smart materials and Structures, 16 (2007) R1.
[10] S.P. Beeby, M.J. Tudor, N.M. White, Energy harvesting vibration sources for microsystems applications, Measurement science and technology, 17 (2006) R175.
[11] K.A. Cook-Chennault, N. Thambi, A.M. Sastry, Powering MEMS portable devices—a review of non-regenerative and regenerative power supply systems with special emphasis on piezoelectric energy harvesting systems, Smart materials and structures, 17 (2008) 043001.
[12] K. Fan, B.o. Yu, L. Tang, Scavenging energy from human limb motions, in: Active and Passive Smart Structures and Integrated Systems 2017, International Society for Optics and Photonics, 2017, pp. 101642P.
[13] M.F. Daqaq, R. Masana, A. Erturk, D.Q. D., On the role of nonlinearities in vibratory energy harvesting: a critical review and discussion, Applied Mechanics Reviews, 66 (2014).
[14] F. Cottone, H. Vocca, L. Gammaitoni, Nonlinear energy harvesting, Physical review letters, 102 (2009) 080601.
[15] M.A. Karami, D.J. Inman, Equivalent damping and frequency change for linear and nonlinear hybrid vibrational energy harvesting systems, Journal of Sound and Vibration, 330 (2011) 5583-5597.
[16] F.C. Moon, P.J. Holmes, A magnetoelastic strange attractor, Journal of Sound and Vibration, 65 (1979) 275-296.
[17] A. Erturk, J. Hoffmann, D.J. Inman, A piezomagnetoelastic structure for broadband vibration energy harvesting, Applied Physics Letters, 94 (2009) 254102.
[18] A. Erturk, D.J. Inman, Piezoelectric energy harvesting, John Wiley & Sons, 2011.
[19] M.A. Karami, P.S. Varoto, D.J. Inman, Analytical approximation and experimental study of bi-stable hybrid nonlinear energy harvesting system, in: International Design Engineering Technical Conferences and Computers and Information in Engineering Conference, 2011, pp. 265-271.
[20] M.S. Mahmoudi, A. Ebrahimian, A. Bahrami, Higher modes and higher harmonics in the non-contact atomic force microscopy, International Journal of Non-Linear Mechanics, 110 (2019) 33-43.
[21] S.C. Stanton, C.C. McGehee, B.P. Mann, Nonlinear dynamics for broadband energy harvesting: Investigation of a bistable piezoelectric inertial generator, Physica D: Nonlinear Phenomena, 239 (2010) 640-653.
[22] A. Erturk, D.J. Inman, A distributed parameter electromechanical model for cantilevered piezoelectric energy harvesters, Journal of vibration and acoustics, 130 (2008).
[23] M.A. Karami, D.J. Inman, Nonlinear hybrid energy harvesting utilizing a piezo-magneto-elastic spring, in: Active and Passive Smart Structures and Integrated Systems 2010, International Society for Optics and Photonics, 2010, pp. 76430U.
[24] A.H. Nayfeh, H.N. Arafat, Nonlinear response of cantilever beams to combination and subcombination resonances, Shock and vibration, 5 (1998) 277-288.
[25] M.A. Karami, Micro-scale and nonlinear vibrational energy harvesting, in, Virginia Tech, 2012.